A Congested $Ru(dps)_2$ or $Ru(dprs)_2$ Core (dps = di-2-pyridyl sulfide; dprs = di-2-pyrimidinyl sulfide) Promotes Sulfur Inversion of *N*,*S*-Chelate Thioethers Containing CH_2R and 2-Pyridyl or 2-Pyrimidinyl Groups

Giuseppe Tresoldi,*[a] Sandra Lo Schiavo,[a] Santo Lanza,[a] and Paola Cardiano[a]

Keywords: Ruthenium / N ligands / S ligands / Sulfur inversion / Activation barriers

The thioethers L [L = 4-methylbenzyl 2-pyridyl sulfide (**L_1**), 4-chlorobenzyl 2-pyridyl sulfide (**L_2**), 3-chlorobenzyl 2-pyridyl sulfide (**L_3**), 1,4-bis(2-pyridylthiomethyl)benzene (**L_4**), 4-methylbenzyl 2-pyrimidinyl sulfide (**L_5**), and 4-chlorobenzyl 2-pyrimidinyl sulfide (**L_6**)], containing a CH_2R group bonded to the sulfur atom, were prepared and characterized. Compounds **L_1**, **L_2**, **L_3**, and **L_4** reacted with *cis*-Ru(*N*,*N*-dprs)$_2$Cl$_2$ or *cis*-Ru(*N*,*N*-dps)$_2$Cl$_2$ (dprs = di-2-pyrimidinyl sulfide, dps = di-2-pyridyl sulfide) leading to the complexes [Ru(*N*,*N*-dprs)$_2$(*N*,*S*-L)][PF$_6$]$_2$ and [Ru(*N*,*N*-dps)$_2$(*N*,*S*-L)][PF$_6$]$_2$. Similar products were obtained from [Ru(*N*,*N*-dps)$_2$(NO$_2$)(NO)][PF$_6$]$_2$ and **L_5** or **L_6**. As a consequence of the L ligand *N*,*S*-chelation, all the complexes contain the four-membered ring RuSCN(*Ru*–*N*). Since the ruthenium and sulfur atoms are stereogenic centres, with Δ and Λ, and *R* and *S* configurations, respectively, they led to four isomers, including the enantiomers. NMR investigations show that the sulfur inversion produces an exchange between the diastereoisomers Δ*R* and Δ*S*, as well as Λ*S* and Λ*R*. The one-dimensional band-shape analysis of the exchanging methylene proton signals showed that the inversion barriers ($\Delta G^{\ddagger}_{298\,K}$) for the dprs complexes are in the 54.9–53.8 kJ mol^{-1} range, with the two invertomers exhibiting similar abundance. Substitution of dprs with dps affects the relative invertomer population leaving the magnitude of $\Delta G^{\ddagger}_{298\,K}$ (52.0–50.6 kJ mol^{-1}) practically unchanged. Conversely, the substitution of the pyridine thioethers (**L_1**, **L_2**) with pyrimidine thioethers (**L_5**, **L_6**) influences the inversion barriers, and $\Delta G^{\ddagger}_{298\,K}$ values of 47.5 and 47.0 kJ mol^{-1} were found for [Ru(*N*,*N*-dps)$_2$(*N*,*S*-**L_5**)][PF$_6$]$_2$ and [Ru(*N*,*N*-dps)$_2$(*N*,*S*-**L_6**)][PF$_6$]$_2$, respectively. An intramolecular mechanism without any bond rupture is suggested on the basis of the $\Delta S^{\ddagger}$ values (negative or close to zero) and the NMR spectra, temperature-reversible and concentration-independent. The contemporary presence of the congested Ru(*N*,*N*-dps)$_2$ or Ru(*N*,*N*-dprs)$_2$ core and sterically demanding *N*,*S*-coordinated thioether ligands is invoked to explain the low energy barrier of the process. This hypothesis is also corroborated by the different behaviour observed for the complex [Ru(bipy)$_2$(*N*,*S*-**L_1**)][PF$_6$]$_2$.

Introduction

The chemistry of the ruthenium compounds containing 2,2′-bipyridine (bipy), polypyridine and similar ligands has been thoroughly explored over many years. This interest has stemmed mainly for the relevance of this chemistry to photophysical, photochemical, and redox phenomena.

Recently we have focused our attention on the bipy or bipy-like ruthenium(II) complexes in which one or more ligands are replaced by di-2-pyridyl sulfide (dps) or other bipy-like nonplanar ligands,[1−3] with the aim of modifying the chemical and physical properties of the complexes.

The dps ligand can in principle exhibit a variety of bonding modes to metal ions: *N*- or *S*-monodentate, *N*,*N*- or *N*,*S*-chelate and *N*,*N*- or *N*,*S*-bridging. However, normally it functions as an *N*,*N*-chelate ligand, adopting a twisted *N*,*N*-inside conformation.[1−11] The control of the coordination mode of this and similar ligands may be achieved by opportune choice of the starting complex. The complexes Ru(diimmine)$_2$Cl$_2$ (diimmine = bipy or 1,10-phenanthroline or similar ligands) are expected to favour the *N*,*N*-chelation,[12−14] whereas Ru(dps)$_2$Cl$_2$ or other sterically hindering diimmines are expected to give species in which dps exhibits a different bonding mode.[15,16]

As proof of this, the *cis*-Ru(bipy)$_2$ fragment favours the *N*,*N*-chelation of dps,[1] whereas the congested *cis*-Ru(*N*,*N*-dps)$_2$ fragment prevents the *N*,*N*-chelation and leads to *N*,*S*-coordinated dps complexes.[17] The crystal structure of [Ru(*N*,*N*-dps)$_2$(*N*,*S*-dps)][PF$_6$]$_2$·H$_2$O[17] clearly shows the distortion of the RuSCN(*Ru*−*N*) ring as well as the steric hindrance effect on the *N*,*S*-coordinate ligand. [The four-membered ring and the coordinated pyridine ring are almost coplanar whereas the pendant pyridine is rotated by 113.9(2)°.] The above complex and the similar species [Ru(*N*,*N*-dps)$_2$(*N*,*S*-phpys)][PF$_6$]$_2$ and [Ru(*N*,*N*-dprs)$_2$(*N*,*S*-phpys)][PF$_6$]$_2$ (phpys = phenyl pyridyl sulfide; dprs = di-2-pyrimidinyl sulfide), as a consequence of the *N*,*S*-coordination, exhibit a sulfur stereogenic centre (*R* and *S* configura-

[a] Dipartimento di Chimica Inorganica, Chimica Analitica e Chimica Fisica, Università di Messina,
98166 Messina, Italy
Fax: (internat.) + 39-090/393756
E-Mail: Tresoldi@chem.unime.it

Supporting information for this article is available on the WWW under http://www.eurjic.com or from the author.

  1434−1948/02/0101−0181 $ 17.50+.50/0

tions) and a pendant ring. The ^1H and ^{13}C NMR spectra were temperature-dependent and the fluxionality of the complexes was interpreted in terms of restricted rotation of the pendant rings and inversion at the sulfur atom. However, only an estimation of the activation energy data for the restricted rotation was possible due to the complex splitting patterns of the proton signals of the coordinated and pendant rings and the numerous partial overlaps of these signals.

In order to elucidate the mechanism of the sulfur inversion, in this paper we report on the synthesis of a series of the novel thioethers [4-methylbenzyl 2-pyridyl sulfide (**L$_1$**), 4-chlorobenzyl 2-pyridyl sulfide (**L$_2$**), 3-chlorobenzyl 2-pyridyl sulfide (**L$_3$**), 1,4-bis(2-pyridylthiomethyl)benzene (**L$_4$**), 4-methylbenzyl 2-pyrimidinyl sulfide (**L$_5$**), and 4-chlorobenzyl 2-pyrimidinyl sulfide (**L$_6$**)] containing sulfur-bonded CH_2R groups. We also report on their coordination chemistry that leads to the formation of the complexes [Ru(*N*,*N*-dprs)$_2$(*N*,*S*-L)][PF_6]$_2$, and [Ru(*N*,*N*-dps)$_2$(*N*,*S*-L)][PF_6]$_2$.

These tris(chelated) ruthenium complexes containing the *N*,*S*-coordinated thioethers exist as the enantiomers Δ and Λ, and in presence of the stereogenic sulfur atom (configuration *S* and *R*) four isomers can exist (Δ*S*, Δ*R*, Λ*S* and Λ*R*). When the thioether is *N*,*S*-chelated, the two methylene protons of the CH_2R group bonded to the sulfur atom are anisochronous. Their ^1H NMR signals are well separated by other signals and very sensitive to the inversion and racemisation processes.

By NMR studies in acetone two exchanging diastereoisomers were identified and the inversion at the sulfur atom examined. The complex [Ru(bipy)$_2$(*N*,*S*-**L$_1$**)][PF_6]$_2$ was also prepared and, in contrast to the other complexes, its NMR spectra, in the range 200−330 K are temperature-independent and show the presence of two non-exchanging isomers.

Results

Synthesis and Characterization of the 4-Methylbenzyl 2-Pyridyl Sulfide (L$_1$), 4-Chlorobenzyl 2-Pyridyl Sulfide (L$_2$), 3-Chlorobenzyl 2-Pyridyl Sulfide (L$_3$), 1,6-Bis(2-pyridylthiomethyl)benzene (L$_4$), 4-Methylbenzyl 2-Pyrimidinyl Sulfide (L$_5$), and 4-Chlorobenzyl 2-Pyrimidinyl Sulfide (L$_6$)

The novel thioether ligands were prepared by heating equimolar amounts of the appropriate mercapto and bromide derivative [2-sulfanylpyridine and 4-methylbenzyl bromide (**L$_1$**) or 4-chlorobenzyl bromide (**L$_2$**) or 3-chlorobenzyl bromide (**L$_3$**), 2-sulfanylpyrimidine and 4-methylbenzyl bromide (**L$_5$**), or 4-chlorobenzyl bromide (**L$_6$**)] in the presence of K_2CO_3 under reflux in DMF under N_2. Compound **L$_4$** was prepared from 2-sulfanylpyridine and α,α′-dichloro-*p*-xylene (or 2-bromopyridine and α,α′-disulfanyl-*p*-xylene) in a molar ratio of 2:1. The DMF was removed by distillation at 100 Torr. The thioethers were obtained as oils by extraction in CH_2Cl_2. Crystallization from CH_2Cl_2/heptane at room temperature (**L$_1$** and **L$_4$**) or at −18 °C (**L$_2$**, **L$_3$**, **L$_5$**, and **L$_6$**) gave white solids. The structures of these compounds were determined by a combination of elemental analysis and usual spectroscopic techniques. The ^1H and ^{13}C NMR spectroscopic data of the ligands in $(CD_3)_2CO$ are collected in Table 1 with the numbering scheme for proton and carbon assignments.

The pyridine proton signals of **L$_1$**, **L$_2$**, **L$_3$**, and **L$_4$** appear as four multiplets in the δ = 7.04−8.46 range, whereas the pyrimidine signals of **L$_5$** and **L$_6$** appear as a triplet and a doublet at δ = 7.15 and 8.59, respectively. The signals of methylene protons were found as singlets in the range δ = 4.37−4.46.

The ^{13}C signals were easily assigned. The pyridine quaternary carbon signals of **L$_1$**, **L$_2$**, **L$_3$**, and **L$_4$** are observed at δ ≈ 159.0, and other pyridine signals in the range δ = 120.2−150.1. The pyrimidine quaternary carbon signals of **L$_5$** and **L$_6$** are observed at δ ≈ 172.0, and other pyrimidine signals at δ ≈ 117.7 (C^5) and 158.1 (C^6 and C^4).

Synthesis of the Compounds

The air-stable compounds [Ru(*N*,*N*-dprs)$_2$(*N*,*S*-L)][PF_6]$_2$ (L = **L$_1$**, **L$_2$** and **L$_4$**), [Ru(*N*,*N*-dps)$_2$(*N*,*S*-L)][PF_6]$_2$ (L = **L$_1$**, **L$_2$** and **L$_3$**) and [Ru(*N*,*N*-bipy)$_2$(*N*,*S*-**L$_1$**)][PF_6]$_2$ were obtained by the reaction of the appropriate dichlorobis(diimmine) complex with an excess of L in boiling ethanol/water (1:1), followed by addition of aqueous NH_4PF_6. The complexes [Ru(*N*,*N*-dps)$_2$(*N*,*S*-**L$_5$**)][PF_6]$_2$ and [Ru(*N*,*N*-dps)$_2$(*N*,*S*-**L$_6$**)][PF_6]$_2$ were prepared from the nitrosyl compound [Ru(*N*,*N*-dps)$_2$(NO_2)(NO)][PF_6]$_2$.[1] All the complexes were soluble in acetone or acetonitrile and slightly soluble in methanol, ethanol, and water.

Conductivity measurements in acetonitrile solution indicate that these compounds are 1−2 electrolytes. Analytical and selected IR data are given in the Exp. Sect.

Dynamic NMR Studies

Variable-temperature ^1H NMR spectra of the compounds were obtained in $(CD_3)_2CO$ in the range 190−330 K. Selected data are listed in Table 2.

Solution Behaviour of the Complexes [Ru(*N*,*N*-dprs)$_2$(*N*,*S*-L$_1$)][PF_6]$_2$, [Ru(*N*,*N*-dprs)$_2$(*N*,*S*-L$_2$)][PF_6]$_2$ and [Ru(*N*,*N*-dprs)$_2$(*N*,*S*-L$_4$)][PF_6]$_2$

At 205 K the NMR spectra of these complexes show the presence of two slow-exchanging isomers in similar abundance. The spectrum of [Ru(*N*,*N*-dprs)$_2$(*N*,*S*-**L$_1$**)][PF_6]$_2$ is shown in Figure 1 and selected data are listed in Table 2. According to the presence of two isomers (population ratio 53:47) two signals are observed in the methyl region (Figure 1a) at δ = 2.28 and 2.27 (the first signal due to the major isomer). Furthermore, four doublets are observed in the methylene region: two doublets of minor intensity at δ = 5.20 and 4.13 (labelled A and B, respectively) and two doublets of major intensity at δ = 4.64 and 4.00 (labelled C and D, respectively). The H^3 pyridine signals appear (Figure 1b) at an abnormally low frequency (δ = 6.23 and 6.13, the first signal of major intensity) due to the strong shielding effect of the phenyl ring. Some signals partially over-

Table 1. ^1H and ^{13}C NMR spectroscopic data[a] of the new ligands

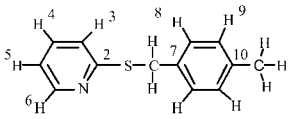

L_1

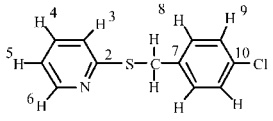

L_2

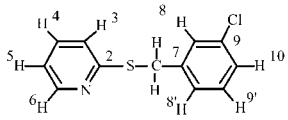

L_3

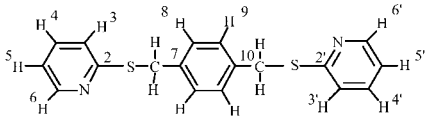

L_4

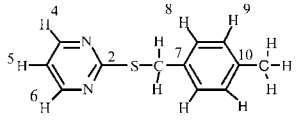

L_5

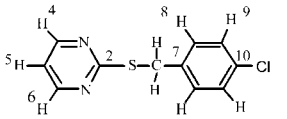

L_6

Ligand	Heterocyclic ring positions						Other positions					
	2	3	4	5	6	7	8	8'	9	10	CH_2	CH_3
L_1		7.21	7.55	7.04	8.45		7.09[b]		7.32[b]		4.44	2.27
	J_{H6H5} = 4.9		J_{H6H4} = 1.9		J_{H6H3} = 1.0							
	J_{H5H4} = 7.4		J_{H5H3} = 1.1		J_{H4H3} = 8.1							
	159.50	122.35	136.80	120.25	150.00	137.10	129.70		129.60	136.00	34.20	22.10
L_2		7.22	7.58	7.07	8.45		7.29[b]		7.44[b]		4.41	
	J_{H6H5} = 5.0		J_{H6H4} = 1.9		J_{H6H3} = 1.0							
	J_{H5H4} = 7.4		J_{H5H3} = 1.1		J_{H4H3} = 8.0							
	158.85	122.55	137.10	120.55	150.10	132.95	131.35		129.05	138.60	34.20	
L_3		7.23	7.60	7.09	8.46		7.39	7.48	7.29	7.23	4.46	
	J_{H6H5} = 5.0		J_{H6H4} = 1.9		J_{H6H3} = 1.0	$J_{H8H8'}$ = 2.0	J_{H8H9} = 6.8		J_{H8H10} = 1.5	J_{H8HCH_2} = 0.6	J_{H9HCH_2} = -0.3	
	J_{H5H4} = 7.4		J_{H5H3} = 1.1		J_{H4H3} = 8.0	$J_{H8'H9}$ = 0.6	$J_{H8'H10}$ = 2.6		J_{H9H10} = 8.0	$J_{H8'HCH_2}$ = 0.6	J_{H10HCH_2} = 0.2	
	158.65	122.55	137.10	120.60	150.10	134.25	129.55	130.65	127.65	128.20	33.35	142.20[c]
L_4		7.22	7.58	7.07	8.44		7.36		7.36		4.42	
	J_{H6H5} = 4.9		J_{H6H4} = 1.9		J_{H6H3} = 1.0							
	J_{H5H4} = 7.4		J_{H5H3} = 1.1		J_{H4H3} = 8.0							
	159.25	122.40	136.95	120.35	150.05	138.00	129.70		129.70	138.00	33.90	
L_5			8.59	7.15	8.59		7.11[b]		7.31[b]		4.37	2.27
			J_{H6H5} = 4.9									
	172.45		158.10	117.65	158.10	137.25	129.70		129.60	135.50	35.10	21.00
L_6			8.59	7.15	8.59		7.30[b]		7.47[b]		4.40	
			J_{H6H5} = 4.9									
	171.85		158.10	117.70	158.10	137.95	131.25		128.90	132.90	35.90	

[a] ^1HNMR spectra recorded at 300.13 MHz and ^{13}C NMR data at 75.56 MHz, T = 298 K in $(CD_3)_2CO$; δ values with respect to internal $SiMe_4$, J_{HH} in Hz. – [b] Unresolved AA'BB' system. – [c] Assigned to $C^{9'}$.

lapped are present in the range δ = 7.20−9.00 whereas in the range δ = 9.00−9.54 the H^6 pyridine and some pyrimidine signals are easily identified.

The almost complete assignment of the signals was based on low-temperature 2D COSY and phase-sensitive 2D NOESY (Figure 2a) experiments. In this way, 24 signals as doublet doublets were assigned to the protons of eight pyrimidine rings with coupling constant J_{45} = 4.60 Hz, J_{46} = 2.15 Hz, and J_{56} = 5.95. In particular, the H^6 pyrimidine protons of the major isomer are observed at δ = 8.79, 8.85, 8.88, and 9.36, while those of the minor isomer at δ = 8.88, 8.81, 9.22, and 9.54.

The 2D NOESY (Figure 2a) was performed at 230 K. At this temperature the significant signals are split and the interchange process is slow. The cross-peaks, due to chemical exchange of magnetization (Figure 2b), are detected between the methylene protons A−D as well as the B−C protons and, in the aromatic region, between the H^3 pyridine protons, between the $H^{6'}$ pyrimidine protons at δ = 9.54 and 9.36 as well as those at δ = 9.22 and 8.88. Figure 2a also shows the negative cross-peaks. The strong NOEs include intra-ring *ortho* interactions (e.g. 6−5, 5−4, and 4−3 in the *N,S*-coordinated pyridine ring and 6−5 in the pyrimidine rings), adjacent-group interactions (e.g. methyl/phenyl protons, not shown in figure, methylene/phenyl protons), and most significantly the following interactions: protons of phenyl ring/H^3 pyridine protons, H^6 pyridine protons and $H^{6'}$ pyrimidine protons at δ = 9.22 and 8.88, methylene proton of the major isomer at δ = 4.64/$H^{6'}$ pyrimidine protons at δ = 9.36. If we assume that there is no restricted rotation, e.g. methylene and phenyl groups freely rotate, since the ruthenium and sulfur atoms are stereogenic

Table 2. Selected ^{1}H NMR spectroscopic data

Complex	T [K][a]	*N,S*-ligand Heterocyclic ring				Other signals[b]				*N,N*-ligands
		H^3	H^4	H^5	H^6	CH_2	CH_2	J [Hz]	CH_3	Selected $H^{6'}$ protons
$[Ru(dprs)_2\mathbf{L_1}][PF_6]_2$	328	6.34	7.89	7.73	9.36	4.53	4.09	12.40	2.32	9.33 8.89
	205	6.23[c]	7.92[c]	7.76[c]	9.43[c]	4.64[c]	4.00[c]	12.45	2.28[c]	9.36[c] 8.88[c]
		6.13	7.87	7.74	9.41	5.20	4.13	12.80	2.27	9.54 9.22
$[Ru(dps)_2\mathbf{L_1}][PF_6]_2$	328	6.27	7.81	7.62	9.24	4.47	3.89	13.00	2.31	9.04 8.72
	205	6.05[c]	7.81[c]	7.64[c]	9.37[c]	5.05[c]	3.73[c]	13.00	2.26[c]	9.24[c] 8.98[c]
		6.17	7.84	7.66	9.34	4.74	3.91	12.55	2.27	9.06 8.57
$[Ru(dprs)_2\mathbf{L_2}][PF_6]_2$	328	6.45	7.92	7.75	9.37	4.58	4.19	12.90		9.32 8.89
	205	6.35	7.93	7.79	9.45	4.67	4.04	12.40		9.34 8.85
		6.28	7.90	7.77	9.41	5.27	4.25	13.10		9.52 9.23
$[Ru(dps)_2\mathbf{L_2}][PF_6]_2$	320	6.40	7.87	7.65	9.28	4.54	4.01	13.45		9.07 8.75
	205	6.23[c]	7.87[c]	7.70[c]	9.39[c]	5.11[c]	3.89[c]	13.10		9.22[c] 9.00[c]
		6.31	7.89	7.72	9.36	4.76	3.98	12.80		9.02 8.57
$[Ru(dps)_2\mathbf{L_3}][PF_6]_2$	328	6.38	7.85	7.64	9.26	4.51	3.99	13.25		9.03 8.72
	210	6.24[c]	7.85[c]	7.68[c]	9.38[c]	5.12[c]	3.86[c]	13.15		9.21[c] 9.00[c]
		6.29	7.87	7.70	9.36	4.77	3.93	12.65		9.03 8.55
$[Ru(dprs)_2\mathbf{L_4}][PF_6]_2$	318	6.28	7.86	7.47	9.39	4.53	4.16	13.00		9.37 8.99
		7.23[e]	7.60[e]	7.08[e]	8.43[e]	4.45[e]				
	210	6.23[c]	7.90[c]	7.77[d]	9.43[c]	4.63[c]	4.02[c]	12.50		9.36[c] 8.81[c]
		6.14	7.85		9.41	5.20	4.17	12.80		9.54 9.20
		7.30[e]	7.62[e]	7.14[e]	8.46[e]	4.41[e]				
$[Ru(dps)_2\mathbf{L_5}][PF_6]_2$	298		8.81	7.74	9.69	4.64	4.35	13.50	2.29	9.08 8.71
	195		8.86[c]	7.80[d]	9.78[c]	5.04[c]	4.34[c]	12.60	2.23[d]	9.29[c] 9.05[c]
			8.90		9.80	4.78	4.39	13.25		[f] [f]
$[Ru(dps)_2\mathbf{L_6}][PF_6]_2$	298		8.78	7.74	9.69	4.71	4.39	13.40		9.09 8.71
	195		8.84[c]	7.80[d]	9.77[c]	5.08[c]	4.40[c]	13.25		9.26[c] 9.03[c]
			8.88		9.80	4.80	4.42	13.25		[f] [f]
$[Ru(bipy)_2\mathbf{L_1}][PF_6]_2$	298	7.43[c]	8.12[c]	7.55[c]	7.88[c]	4.29[c]	3.81[c]	12.55	2.22[c]	9.66[c] 8.76[c]
		7.36	8.13	7.50	7.89	4.71	4.26	13.30	2.18	9.89 8.84

[a] Recorded in $(CD_3)_2CO$ at 300.13 MHz, δ in ppm with respect to internal $SiMe_4$. Coupling constants (Hz) in the pyridine rings: J_{43} = 7.7−8.1, J_{45} = 7.4−7.8, J_{65} = 4.8−5.5, J_{64} = 1.1−1.9, J_{53} = 0.7−1.3, and J_{63} = 0.7−0.8; in the pyrimidine rings: J_{65} = 5.5−6.0, J_{45} = 4.6−5.0, and J_{64} = 2.0−2.1. − [b] The phenyl signals are observed as unresolved AA′BB′ systems in the range δ = 7.2−7.8. − [c] Assigned to the major isomer. − [d] Overlapped signals of the two isomers. − [e] Uncoordinated side. − [f] Not assigned.

centres (configurations Δ and Λ, *R* and *S*, respectively), the complex has a total of four isomers including the enantiomers. Thus, the above-mentioned positive and negative cross-peaks found in the 2D NOESY imply that in the two isomers (Figure 3) the phenyl protons, in *ortho* positions with respect to the methylene group, are in close proximity to the H^3 pyridine protons (in Figure 3 only a phenyl *ortho*-proton is shown). Furthermore, the H^6 pyridine proton is in close proximity to the H^6 pyrimidine proton at δ = 8.88 (major isomer) or that at δ = 9.22 (minor isomer). Moreover, in the major isomer the methylene protons are in close proximity to the $H^{6'}$ pyrimidine proton at δ = 9.36. These results are indicative of a sulfur inversion, which exchanges the two diasteroisomers $\Delta R \rightleftarrows \Delta S$ (or $\Lambda S \rightleftarrows \Lambda R$), as depicted in Figure 3.

On warming the NMR solutions, all the spectral lines broaden. In particular the coalescence for the exchange $A \rightleftarrows D$ and $B \rightleftarrows C$ occurred around 280 K.

At 330 K, the highest temperature reached, two averaged methylene doublets and a single methyl signal were observed (Table 2). It is pertinent to note at this point that the splitting patterns of methylene protons, at high temperature, definitely eliminate the possibility of racemisation ($\Delta \rightleftarrows \Lambda$). In fact, in presence of a fast inversion and racemisation the averaged environments of the methylene protons should become equivalents. Furthermore, EXSY experiments in the range 300−330 K exclude a slow racemisation process. The complete assignment of the signals was performed with the help of the COSY spectrum. In the aromatic region, at this temperature, twelve pyrimidine proton signals due to four rings of the *N,N*-coordinated ligands are observed. In particular, the signals at δ = 9.33, 8.89 and 8.70 (two overlapped signals) were assigned to the H^6 pyrimidine protons, while four pyridine proton signals of the *N,S*-coordinated ligand are detected (Table 2).

The rates of the processes were deduced by band-shape analysis of the methylene signals, which are well separated by other signals and very sensitive to the process by virtue of the methylene closeness to the site of inversion. Some experimental and computer-simulated spectra are shown in Figure 4. As evident from the figure, the shifts are found to be strongly temperature-dependent. In order to correct for this temperature dependence a linear interpolation was used.[18] The resulting rate data were checked on the H^3 pyridine signals. Activation energy data were calculated from 16 independent fittings in the temperature range 205−330 K. Activation energy data for the other dprs com-

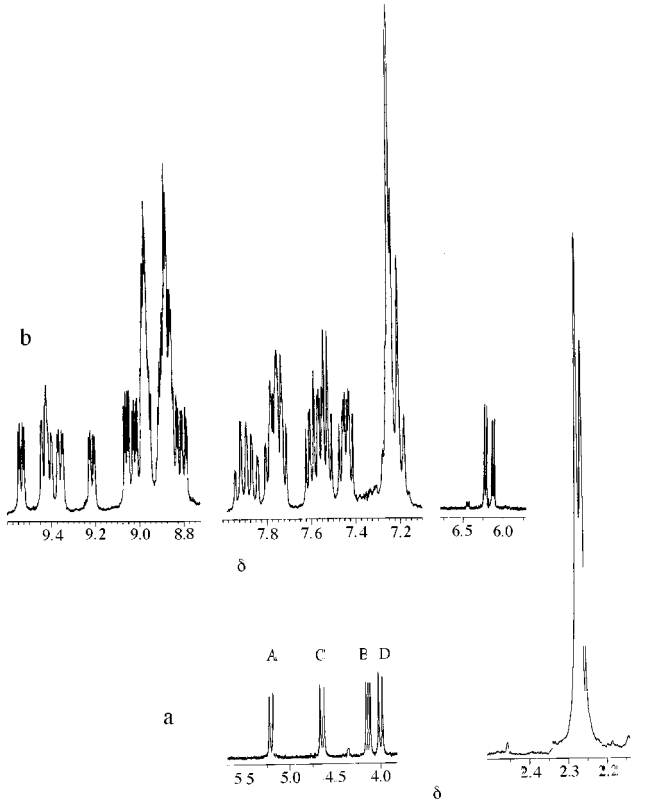

Figure 1. ^{1}H NMR spectrum of [Ru(*N,N*-dprs)$_2$(*N,S*-L$_1$)][PF$_6$]$_2$ at 205 K in (CD$_3$)$_2$CO; a) methylene and methyl region, b) aromatic region

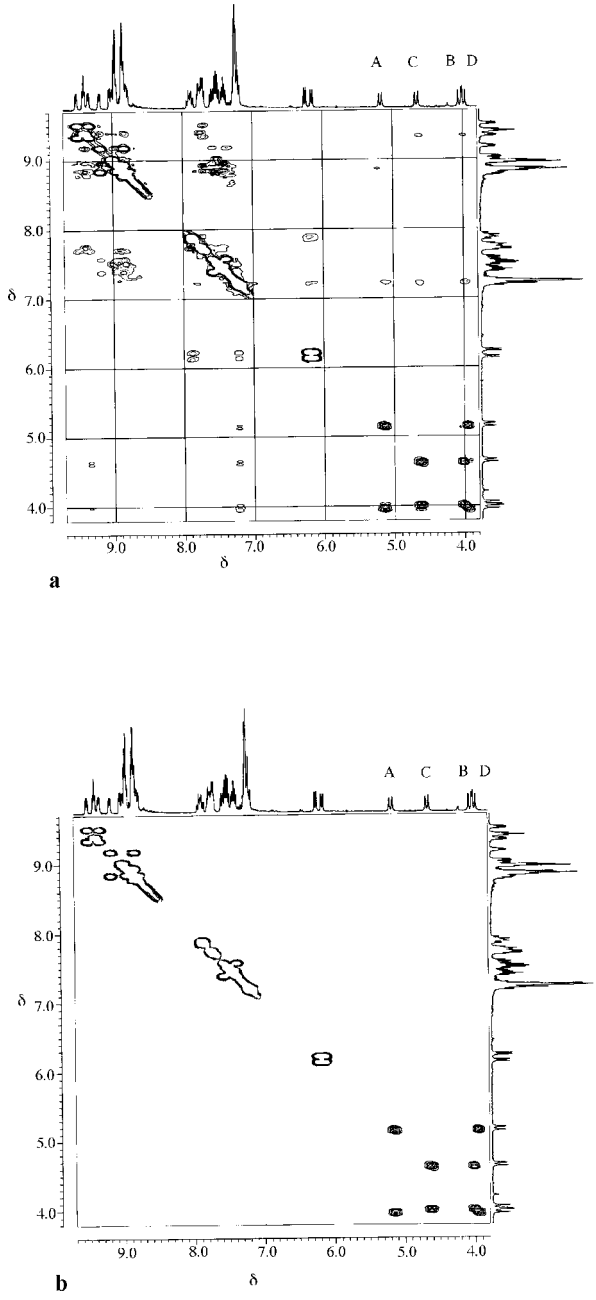

Figure 2. Phase-sensitive 2D NOESY of [Ru(*N,N*-dprs)$_2$(*N,S*-**L$_1$**)][PF$_6$]$_2$ at 230 K in (CD$_3$)$_2$CO; a) positive and negative cross-peaks, b) only positive cross-peaks

plexes were obtained by similar method and collected in Table 3.

The ^{13}C NMR spectra were easily interpreted, at least for the carbon signals of the *N,S*-ligand, by comparison of the spectra of the present complexes with those of the free ligands and other complexes containing *N,S*-chelated ligands,[17] with the help of CH-correlation experiments and jmod pulse sequences. ^{13}C NMR spectra of all three dprs complexes were similar (Table 4) and the results for [Ru(dprs)$_2$(*N,S*-**L$_1$**)][PF$_6$]$_2$ will serve to illustrate the analysis of the problem.

The ^{13}C NMR spectrum at 228 K comprised three regions of interest for the *N,S*-chelate ligand: (i) the methyl region that displayed the methyl resonances of the two isomers as overlapped signals at δ = 19.95; (ii) the methylene region with two signals at δ = 38.70 and 40.20 (the latter of the major isomer); (iii) the phenyl and pyridyl region (δ = 165−126) in which the C^7 quaternary carbon atoms of the two isomers are observed as overlapped signals. The C^3 pyridine carbon atom of the minor isomer and C^5 pyridine carbon atom of the major isomer led to superimposed signals whereas other resonances are well separated.

On warming the NMR solutions above 245 K some signals broaden, and in the range 265−285 K some signals vanish (in particular the methylene signals). In the fast exchange regime (328 K) averaged signals of the two isomers were observed (Table 4).

In the ^{13}C NMR spectrum of [Ru(dprs)$_2$(*N,S*-**L$_4$**)][PF$_6$]$_2$ the **L$_4$** carbon signals of the uncoordinated pyridyl ring and of the methylene group in the uncoordinated side are also observed. These signals and the corresponding signals of the free ligand show, at the same temperature, nearly the same chemical shift.

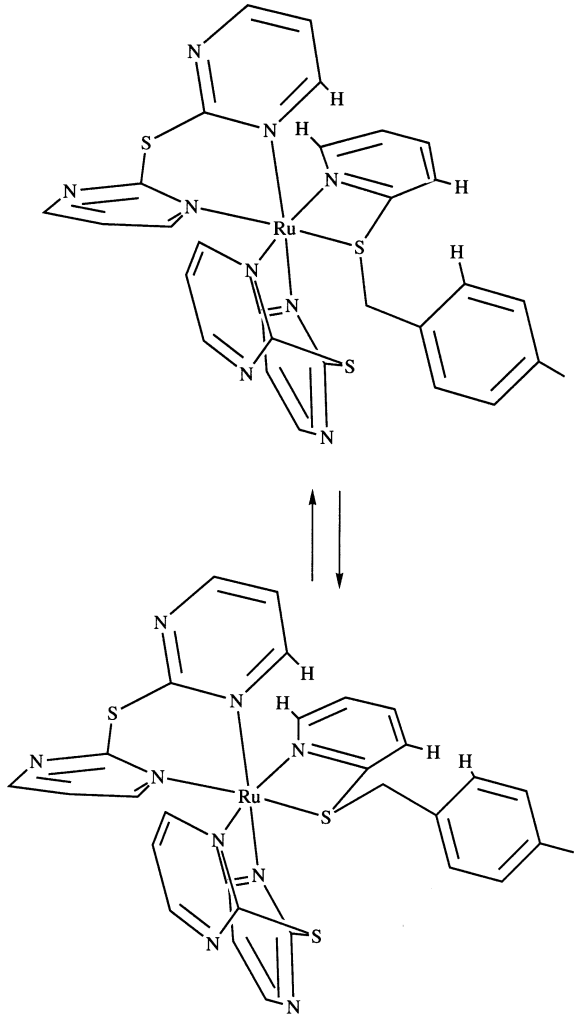

Figure 3. Schematic representation of the proposed structure for the diastereoisomers of $[Ru(N,N\text{-dprs})_2(N,S\text{-}\mathbf{L_1})][PF_6]_2$ and of the close proximity between the phenyl *ortho*-protons (only one is shown) and H^3 pyridine protons and that between the H^6 pyridine protons and H^6 pyrimidine proton at $\delta = 8.88$ (major isomer) or at $\delta = 9.22$ (minor isomer)

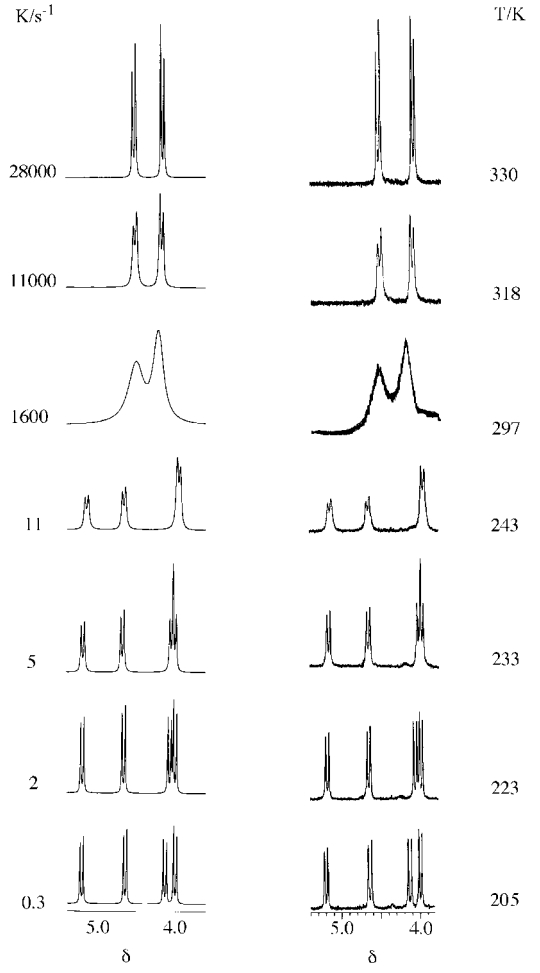

Figure 4. Selected variable-temperature ^1H NMR spectra of $[Ru(N,N\text{-dprs})_2(N,S\text{-}\mathbf{L_1})][PF_6]_2$ at 205 K in $(CD_3)_2CO$ (methylene region); computer-synthesised spectra of the same region are shown on the left

Solution Behaviour of the Complexes $[Ru(dps)_2(N,S\text{-}\mathbf{L_1})][PF_6]_2$, $[Ru(dps)_2(N,S\text{-}\mathbf{L_2})][PF_6]_2$ and $[Ru(dps)_2(N,S\text{-}\mathbf{L_3})][PF_6]_2$

Also for these complexes, two slow-exchanging isomers are present at 205 K, but the population ratio between the isomers is ca. 2:1 (Table 3). Furthermore, the methylene proton signals appear different with respect to those of the $[Ru(dprs)_2(N,S\text{-L})][PF_6]_2$ complexes in that now the methylene signals (Figure 5) of the minor isomer (C and D) are framed by those of the major isomer (A and B).

The 2D ^1H NOESY experiment on $[Ru(dps)_2(N,S\text{-}\mathbf{L_2})][PF_6]_2$ is shown in Figure 5. The positive cross-peaks show the chemical exchange between the methylene protons (A−D and B−C), between the H^6 pyrimidine protons at $\delta = 9.00$ and 8.57 (the first signal of major intensity), and between the H^6 pyrimidine protons at $\delta = 9.22$ and 9.02 (the first signal of major intensity). The most significant negative cross-peaks show strong NOEs due to the close proximity of phenyl protons and H^3 pyridine protons of *N*,*S*-chelated ligand and between the H^6 pyridine protons of *N*,*S*-chelated ligand and the H^6 pyridine protons of *N*,*N*-chelated ligands at $\delta = 9.00$ and 8.57, respectively. Thus, also in this case there are two exchanging diastereoisomers. In the major isomer the phenyl protons are in close proximity to the H^3 proton at $\delta = 6.23$ and in the minor isomer of the H^3 proton at $\delta = 6.31$. Rates of the process were deduced by band-shape analysis of the methylene signals. Also in this case a linear interpolation was necessary due to the strong temperature dependence of the signals. Activation energy data were collected in Table 3.

Solution Behaviour of the Complexes Containing Pyrimidine Thioethers as N,S-Ligands: $[Ru(dps)_2(N,S\text{-}\mathbf{L_5})][PF_6]_2$ and $[Ru(dps)_2(N,S\text{-}\mathbf{L_6})][PF_6]_2$

In contrast to the complexes containing pyridine thioethers as *N*,*S*-ligands, which showed some broad signals at room temperature (in particular broad methylene signals, see Figure 4), the ^1H NMR spectra of these complexes showed well-resolved signals in agreement with the presence

Table 3. Activation energy data

	Population (%)	$\Delta G^{\#}_{298\,K}$ [kJ mol^{-1}]	$\Delta H^{\#}$ [kJ mol^{-1}]	$\Delta S^{\#}$ [J K^{-1}mol^{-1}]
$[Ru(dprs)_2\mathbf{L_1}](PF_6)_2$	53:47	54.1 ± 0.2	48.9 ± 1.9	−17.4 ± 7.0
$[Ru(dprs)_2\mathbf{L_2}](PF_6)_2$	50:50	53.8 ± 0.1	44.9 ± 3.0	−30.0 ± 8.0
$[Ru(dprs)_2\mathbf{L_4}](PF_6)_2$	53:47	54.9 ± 0.2	49.2 ± 2.5	−19.2 ± 9.0
$[Ru(dps)_2\mathbf{L_1}](PF_6)_2$	60:40	51.8 ± 0.2	49.3 ± 1.6	−8.2 ± 5.9
$[Ru(dps)_2\mathbf{L_2}](PF_6)_2$	66:34	52.0 ± 0.6	53.1 ± 1.6	+3.4 ± 4.0
$[Ru(dps)_2\mathbf{L_3}](PF_6)_2$	67:33	50.6 ± 0.3	52.2 ± 1.8	+5.3 ± 7.0
$[Ru(dps)_2\mathbf{L_5}](PF_6)_2$	65:35	47.5 ± 0.5	40.0 ± 2.0	−25.0 ± 5.0
$[Ru(dps)_2\mathbf{L_6}](PF_6)_2$	65:35	47.0 ± 0.5	39.5 ± 2.0	−24.0 ± 5.0

Table 4. Selected ^{13}C NMR spectroscopic data

Complex	T [K][a]	*N,S*-coordinated ligand										
		Heterocyclic ring					Phenyl ring[b]				CH_2	CH_3
		C^2	C^3	C^4	C^5	C^6	C^7	C^8	C^9	C^{10}		
$[Ru(dprs)_2\mathbf{L_1}][PF_6]_2$	328	165.05	128.45	140.55	127.80	157.35	140.05	130.90	130.75	131.55	42.05	21.20
	228	163.25[c]	127.20[c]	138.65[c]	126.00[c]	155.60[c]	138.10[d]	129.40[c]	129.35[c]	130.55[c]	40.20[c]	19.95[d]
		164.40	126.10	138.95	126.20	155.40		129.50	129.25	131.10	38.70	
$[Ru(dps)_2\mathbf{L_1}][PF_6]_2$	328	164.95	127.70	139.75	126.85	157.90	139.75	130.85	130.60	131.80	42.40	21.15
	218	163.70[c]	127.30[c]	138.65[d]	125.95[c]	156.10[c]	137.65[d]	129.25[d]	128.90[c]	131.25[c]	40.60[c]	19.75[d]
		162.85	127.10		126.05	156.05			129.00	130.60	38.20	
$[Ru(dprs)_2\mathbf{L_2}][PF_6]_2$	320	164.60	128.30	140.60	127.75	157.20	135.20	132.45	130.00	133.65	41.00	
	228	164.15	127.35	139.20	126.35	155.70	133.40[d]	131.32	128.80	132.80[d]	39.45	
		162.90	126.35	138.90	126.15	155.45		131.20	128.70		38.10	
$[Ru(dps)_2\mathbf{L_3}][PF_6]_2$	320	164.55	127.65	139.85	127.10	158.00	137.55	130.35	135.20	129.30	41.50	
								130.15	129.35			
	218	163.50[c]	127.40[c]	138.75[d]	126.00[c]	156.15[c]	137.10[c]	128.35[c]	133.20[d]	127.90[d]	39.85[c]	
		162.35	127.15		126.40	156.25	136.40	128.20	127.90[d]		37.70	
$[Ru(dprs)_2\mathbf{L_4}][PF_6]_2$	318	165.10	128.50	140.60	127.90	157.45	141.10	131.10	130.80	136.30	42.00	
		159.20[e]	122.65[e]	137.40[e]	120.90[e]	150.40[e]					34.05[e]	
	228	163.30[c]	127.05[c]	138.65[d]	126.00[c]	155.60[c]	139.00[d]	129.50[c]	129.40[c]	132.50[c]	40.05[c]	
		164.45	126.20		126.05	155.35		129.60	129.25	133.00	38.50	
		157.35[e]	121.15[e]	136.15[e]	119.45[e]	148.90[e]					32.05[e]	
$[Ru(dps)_2\mathbf{L_5}][PF_6]_2$	298	174.00		159.35	122.85	165.35	138.65	130.35	129.95	132.15	40.10	20.75
	195	173.45[c]		159.35[c]	121.40[d]	163.80[c]	137.50[c]	129.20[c]	128.30[d]	131.85[d]	40.00[c]	19.45[c]
		172.80		158.45		163.85	137.70	129.30			38.00	19.35
$[Ru(dps)_2\mathbf{L_6}][PF_6]_2$	298	174.10		159.50	123.10	165.50	138.80	132.45	130.10	133.00	39.65	
	195	173.45[c]		159.35[c]	121.70[d]	163.85[c]	137.80[c]	130.35[c]	129.10[c]	132.00[d]	39.65[c]	
		172.45		158.45		163.75		130.45	129.00		37.00	
$[Ru(bipy)_2\mathbf{L_1}][PF_6]_2$	298	162.25[c]	128.55[c]	140.00[c]	125.20[c]	154.00[c]	138.85[c]	129.95[d]	128.85[c]	130.10[d]	38.25[c]	20.60[c]
		162.20	127.50	137.60	125.80	153.75	138.75		128.90		35.75	20.50

[a] Recorded in $(CD_3)_2CO$ at 75.56 MHz. – [b] Assignments of the quaternary phenyl carbon atoms C^7 and C^{10} possibly reversed. – [c] Assigned to the major isomer. – [d] Overlapped signals of the two isomers. – [e] Uncoordinated side.

of two fast-exchanging isomers (Figure 6). Unluckily, experimental difficulties ruled out the possibility of performing one- and two-dimensional experiments below 190 K. At this temperature the signal broadening, due to the inversion process, was not negligible and prevented the assignment of most signals. However, the band-shape analysis of the methylene signals above 190 K allows the evaluation of the activation energies. According to the fast inversion observed at room temperature, the mean values of the activation barriers, $\Delta G^{\ddagger}$ and $\Delta H^{\ddagger}$, for these complexes were 47.2 and 39.7 kJ mol^{-1}, respectively, whereas for the corresponding complexes containing thioarylpyridine as *N,S*-ligands (e.g. $[Ru(dps)_2(N,S\text{-}\mathbf{L_1})][PF_6]_2$ and $[Ru(dps)_2(N,S\text{-}\mathbf{L_2})][PF_6]_2$) the mean values were 52.9 and 49.6 kJ mol^{-1}, respectively.

Although some carbon signals (in particular of the minor isomer) were not observed in the slow exchange regime, the ^{13}C NMR spectra (Table 4) of $[Ru(dps)_2\,L][PF_6]_2$ complexes (L = $\mathbf{L_1}$, $\mathbf{L_2}$, $\mathbf{L_3}$, $\mathbf{L_5}$, and $\mathbf{L_6}$) confirm the presence of the two exchanging isomers.

Discussion

Our previous studies[17] on the dynamic behaviour of $[Ru(N,N\text{-dprs})_2(N,S\text{-phpys})][PF_6]_2$ and $[Ru(N,N\text{-dps})_2(N,S$-

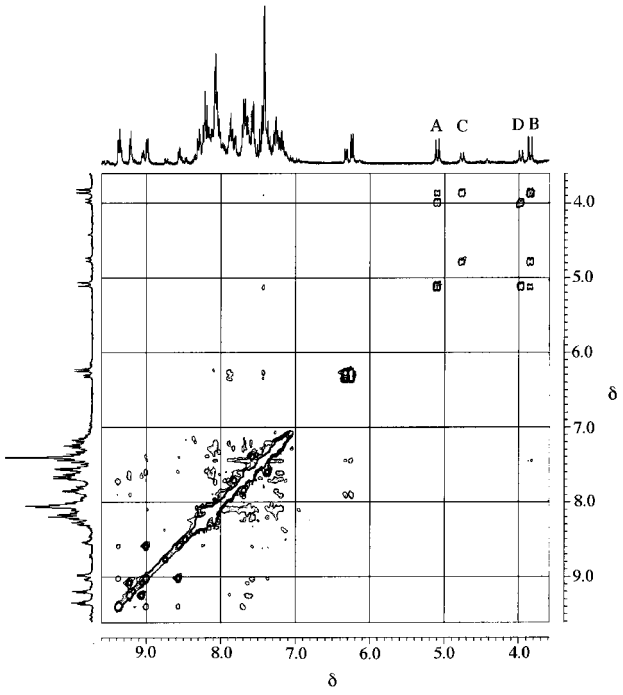

Figure 5. Phase-sensitive 2D NOESY of [Ru(*N*,*N*-dps)$_2$(*N*,*S*-**L$_2$**)][PF$_6$]$_2$ at 218 K in (CD$_3$)$_2$CO; positive and negative cross-peaks are shown

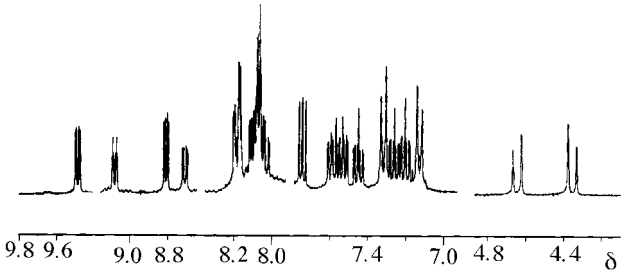

Figure 6. ^{1}H NMR spectrum of [Ru(*N*,*N*-dps)$_2$(*N*,*S*-L$_5$)][PF$_6$]$_2$ at 298 K in (CD$_3$)$_2$CO

phpys)][PF$_6$]$_2$ (phpys = phenyl pyridyl sulfide) show, in the range 180−240 K, that a restricted rotation of the pendant phenyl ring was operative, affecting only the phenyl proton signals. Above 240 K extensive internal arrangements, involving sulfur inversion were invoked to explain the higher temperature changes in the aromatic region of ^{1}H NMR spectra.

In contrast, the NMR spectra of the present complexes, at the lower temperatures reached (190 K), clearly show the presence of two slow-exchanging invertomers and the absence of any restricted rotation. Very likely, restricted rotation of the methylene or phenyl group occurs below the above temperature, but experimental difficulties ruled out the possibility of supporting this suggestion. Thus, the present tris(chelated) ruthenium complexes containing the ruthenium chiral atom (configurations Δ and Λ) and the sulfur chiral atom (configurations *S* and *R*) can exist only as four isomers. The process consistent with the NMR behaviour is the inversion at the sulfur atom ($R \rightleftarrows S$), whereas the possibility of racemisation ($\Delta \rightleftarrows \Lambda$) can be discarded.

The inversion at the sulfur atom may occur through one of three processes: a) a dissociative mechanism; b) a mechanism involving association of solvent or anion or free ligand; or c) intramolecular mechanism without any bond rupture. A dissociative mechanism with sulfur or nitrogen decoordination is unlikely on the basis of the $\Delta S^{\ddagger}$ values and ^{1}H NMR spectra, which are temperature-reversible and concentration-independent.

In particular, for the complexes containing pyrimidine thioether ligands, the dissociative mechanism may involve exchange of the coordinated and uncoordinated N-atoms through dissociation of the ruthenium−N bond, rotation around the pyrimidine−S bond, inversion at the sulfur atom and reformation of the pyrimidine−ruthenium bond. This mechanism can be definitively rejected in that it should make the H^6 and H^4 pyrimidine protons equivalent, whereas the latter protons are nonequivalent even when the process becomes fast at the NMR time scale. A dissociative mechanism involving nitrogen decoordination in the pyridine thioethers complexes can also be discarded on the basis of the pyridine basicity (pK_a = 5.25) being much larger than that of the pyrimidine (pK_a = 1.23), which suggests better σ-donor capability of the pyridine.

Even though the determination of $\Delta S^{\ddagger}$ values is based on extrapolation to $1/T = 0$ in the Eyring diagrams and, owing to the long distance over which this extrapolation has to be taken, is subject to considerable uncertainty, the data collected show that the activation entropies for [Ru(*N*,*N*-dprs)$_2$(*N*,*S*-L)][PF$_6$]$_2$ (L = **L$_1$**, **L$_2$**, and **L$_4$**) and [Ru(*N*,*N*-dps)$_2$(*N*,*S*-L)][PF$_6$]$_2$ (L = **L$_5$** and **L$_6$**) are, without doubt, negative (Table 3). Thus, the transition state conformations should be sterically even more congested than the ground state conformations, suggesting that a dissociative mechanism can be discarded. For [Ru(*N*,*N*-dps)$_2$(*N*,*S*-L)][PF$_6$]$_2$ (L = **L$_1$**, **L$_2$**, and **L$_3$**), the activation entropies are -8.2 ± 5.9 J K^{-1} mol^{-1}, $+3.4 \pm 4.0$ J K^{-1} mol^{-1}, and $+5.3 \pm 7.0$ J K^{-1} mol^{-1}, respectively. Although these values, different to those of other complexes, are close to zero, it is pertinent to note that the $\Delta G^{\ddagger}_{298\,K}$ values for the process in the corresponding dprs and dps complexes (Table 3) are of comparable magnitude, strongly suggesting that a similar mechanism is operative.

On the other hand, a mechanism involving association of solvent or anion or free ligand can be discarded on the basis of the following NMR findings: (i) the ^{1}H NMR spectra are temperature-reversible and concentration-independent; (ii) when free ligand is added separate signals are observed and the exchange rates are not affected; (iii) for the complex [Ru(dprs)$_2$(*N*,*S*-**L$_4$**)][PF$_6$]$_2$ the presence of the uncoordinated side in the thioether ligand does not affect the process; and (iv) addition of chloride or hexafluorophosphate anion does not affect the exchange rate.

The only mechanism, therefore, consistent with all the experimental results appears to be the pyramidal inversion without any bond rupture. However, the inversion barriers for the present complexes are low with respect to those

found in iron or ruthenium complexes containing bridging[19] or chelating[20] ligands, and other complexes containing *N,S*-coordinated ligands that form five-membered chelate rings.[21,22] Furthermore, decreasing the size of the ring containing the sulfur atom ought to make the access to the planar transition state more difficult, with a consequent increase in the pyramidal inversion energy barrier.[20]

The low $\Delta G^{\ddagger}$ values of the present complexes, which reflect differences between the ground- and transition-state energy, are mainly due to relatively high-energy ground states rather than low-energy transition states. This may be explained in terms of the contemporary presence of the congested Ru(*N,N*-dps)$_2$ or Ru(*N,N*-dprs)$_2$ fragments and steric demanding thioether ligands *N,S*-coordinated. This hypothesis is supported by the NMR spectra of the [Ru(bipy)$_2$(*N,S*-**L$_1$**)][PF$_6$]$_2$ that show the presence of two non-exchanging isomers, even at the highest temperatures achievable in acetone. The planar disposition of the bipy ligands in the last complex very likely reduces the steric hindrance of the [Ru(*N,N*-diimmine)$_2$ fragment and the ground-state energy with consequent increase of the $\Delta G^{\ddagger}$ value.

Conclusion

The synthesis of a series of novel thioethers bearing CH_2R groups allowed us to extend the chemistry of polypyridine ruthenium(II) compounds containing *N,S*-coordinated ligands with a four-membered chelate ring, and to elucidate the sulfur inversion mechanism. The pyramidal inversion, without bond rupture, is likely to be the only mechanism consistent with the dynamic behaviour of the present complexes. The steric hindrance of the ruthenium substrates and the steric demand of the thioether ligand *N,S*-coordinated appear to play a determinant role for the inversion process.

The process occurs at distinctly lower rates in the complexes containing pyridine thioethers (**L$_1$**, **L$_2$**, **L$_3$**, **L$_4$**) than in those containing pyrimidine derivatives (**L$_5$**, **L$_6$**), the differences in the averaged $\Delta G^{\ddagger}$ values being 8 kJ mol^{-1}. Steric and electronic effects may be invoked to explain this difference. In fact, the pyridine H^3 proton, in close proximity to the phenyl ring in the *N,S*-coordinated ligand, should increase the energy barrier of the dynamic process. On the other hand, the substitution in the thioether ligand of the pyridine with pyrimidine should weaken the ruthenium−sulfur bond (pyrimidine is a better electron-withdrawing group than pyridine) and decrease the energy barrier. Further attempts are in progress with the aim to study the effect of more or less congested Ru(*N,N*-diimine)$_2$ cores on the structure of the isomers and the exchange process.

Experimental Section

Di-2-pyridyl sulfide,[24] [Ru(dps)$_2$Cl$_2$]·2H$_2$O,[1] [Ru(dprs)$_2$Cl$_2$]·2H$_2$O,[17] and [Ru(dps)$_2$(NO)(NO$_2$)][PF$_6$]$_2$·H$_2$O[1] were prepared by published methods. Other reagents and solvents were used as received. − Elemental analyses were carried by Redox Microanalytical Laboratory of Cologno Monzese (Milano). − Conductivity measurements were done with a Radiometer CDM 3 conductivity meter. − Infrared spectra were recorded with an FT-IR 1720X spectrophotometer with samples as Nujol mulls placed between KBr plates. − The ^{1}H and ^{13}C NMR spectra were recorded with a Bruker AMX 300 spectrometer. The following Bruker programs were used: zg, homodecnew, zgpg, jmod, cosy, noesy.pt, hxco, invb. Simulations of static and dynamic spectra were performed using the G NMR program.

4-Methylbenzyl 2-Pyridyl Sulfide (L$_1$): The compounds 2-sulfanylpyridine (11.1 g, 0.1 mol), 4-methylbenzyl bromide (18.5 g, 0.1 mol), and potassium carbonate (11.0 g, 0.08 mol) were vigorously stirred in dimethylformamide (40 cm^3), and heated under reflux for 5 h, under N_2. The dimethylformamide was then distilled under reduced pressure (100 Torr) and the residue extracted with CH_2Cl_2 (ca. 250 cm^3). To the solution was added aluminium oxide (activated neutral, STD grade, 10 g). The mixture was allowed to stand until the solution was almost colourless (ca. 1 d). By evaporation of the filtered solution, a pale yellow oil was obtained that was dissolved in 150 cm^3 of CH_2Cl_2/heptane (1:2). A white solid was formed by slow concentration. Yield 11.0 g (51%). − Selected IR data (KBr): $\tilde{\nu}$ = 1578 vs, 1557 s, 1515 s, 1454 vs, 1415 vs, 1124 vs, 841 br, 758 vs, 740 ms, 726 s cm^{-1}. − $C_{13}H_{13}NS$ (215.31): calcd. C 72.50, H 6.10, N 6.50, S 14.90; found C 72.60, H 6.15, N 6.55, S 14.90.

4-Chlorobenzyl 2-Pyridyl Sulfide (L$_2$): This compound was obtained starting from 2-sulfanylpyridine (11.1 g, 0.1 mol), 4-chlorobenzyl chloride (16.1 g, 0.1 mol), and potassium carbonate (11.0 g, 0.08 mol) in dimethylformamide (40 cm^3) under reflux for 7 h, under N_2. After removal of the DMF, extraction with CH_2Cl_2 (ca 250 cm^3), and addition of aluminium oxide (10 g), the mixture was allowed to stand until the solution was colourless. The filtered solution was concentrated to give an oil that was kept at −24 °C. Colourless needles were formed. Yield 10.0 g (42%). − Selected IR data (KBr): $\tilde{\nu}$ = 1578 vs, 1556 vs, 1490 vs, 1453 vs, 1414 vs, 1122 vs, 1091 vs, 1015 vs, 853 br, 756 vs, 730 s, 725 s cm^{-1}. − $C_{12}H_{10}ClNS$ (235.73) calcd: C 61.15, H 4.30, N 5.95, S 13.60; found C 61.10, H 4.35, N 6.00, S 13.60.

3-Chlorobenzyl 2-Pyridyl Sulfide (L$_3$): This white compound was obtained in the same manner as above, starting from 2-sulfanylpyridine (11.1 g, 0.1 mol), 3-chlorobenzyl bromide (20.5 g, 0.1 mol), and potassium carbonate (11.0 g, 0.08 mol). Reaction time: 3 h. Yield 8.0 g (34%). − Selected IR data (KBr): $\tilde{\nu}$ = 1597s, 1579 vs, 1556 vs, 1453 vs, 1414 vs, 1123 vs, 876 br, 787 br, 757 vs, 725 vs cm^{-1}. − $C_{12}H_{10}ClNS$ (235.73): calcd. C 61.15, H 4.30, N 5.95, S 13.60; found C 61.20, H 4.35, N 6.00, S 13.70.

1,4-Bis[(phenylsulfanyl)methyl]benzene (L$_4$): The compounds 2-bromopyridine (15.8 g, 0.1 mol), 1,4-benzenedimethanethiol (8.52 g, 0.05 mol), and potassium carbonate (11 g, 0.08 mol) were vigorously stirred in dimethylformamide (40 cm^3) and heated under reflux for 5 h. The solvent was then removed ant the resulting brown solid extracted with a mixture (210 cm^3) of CH_2Cl_2 and heptane (1:2). The first crop of solid separated by slow evaporation (ca. 2 h) as a white pure product. To the solution was added the residue, CH_2Cl_2 (100 cm^3), and aluminium oxide (activated neutral, STD grade, 10 g). The mixture was allowed to stand until the solution was almost colourless (ca. 1 d). By slow concentration of the filtered solution the second crop of product was obtained. Total yield 19.5 g (60%). − Selected IR data (KBr): $\tilde{\nu}$ = 1576 vs, 1550 s, 1514 s, 1121 vs, 894 s, 823 s, 757 vs, 732 s, 724 vs, 504s cm^{-1}. −

$C_{18}H_{16}N_2S_2$ (324.46): calcd. C 66.65, H 4.95, N 8.65, S 19.75; found C 66.60, H 5.00, N 8.55, S 19.70. − Compound **L_4** was also obtained in the same way starting from 2-sulfanylpyridine (11.3 g, 0.1 mol) and α,α′-dichloro-*p*-xylene (8.75 g, 0.05 mol). Yield ca. 50%.

4-Methylbenzyl 2-Pyrimidinyl Sulfide (L_5): This white compound was obtained as like **L_2** from 2-sulfanylpyrimidine (11.2 g, 0.1 mol), 4-methylbenzyl bromide (18.5 g, 0.1 mol), and potassium carbonate (11.0 g, 0.08 mol). Yield 10.6 g (49%). − Selected IR data (KBr): $\tilde{\nu}$ = 1565 vs, 1546 vs, 1516 s, 1205 s, 1181 s, 1170 s, 803 s, 771 vs, 757 ms, 744 s. 727s cm^{-1}. − $C_{12}H_{12}N_2S$ (216.30): calcd: C 66.65, H 5.60, N 12.95, S 14.80; found C 66.60, H 5.65, N 12.85, S 14.90.

4-Chlorobenzyl 2-Pyrimidinyl Sulfide (L_6): This white compound was obtained like **L_2** from 2-sulfanylpyrimidine (11.2 g, 0.1 mol), 4-chlorobenzyl chloride (16.1 g, 0.1 mol), and potassium carbonate (11.0 g, 0.08 mol). Yield 10.6 g (45%). − (KBr): $\tilde{\nu}$ = 1566 vs, 1548 vs, 1490 s, 1206 s, 1184 s, 1159 s, 1093 vs, 1015 s, 812 s, 769 s, 750 vs, 722 s cm^{-1}. − $C_{11}H_9ClN_2S$ (236.72): calcd. C 55.80, H 3.85, N 11.85, S 13.55; found C 55.80, H 3.95, N 11.80, S 13.60.

$[Ru(dprs)_2(L_1)][PF_6]_2$: $[Ru(dprs)_2Cl_2]\cdot 2H_2O$ (0.196 g, 0.33 mmol) and **L_1** (0.190 g, 0.882 mmol) were heated under reflux in 60 cm^3 of ethanol/water (1:1). After 1 h, the red complex was dissolved and the yellow solution was filtered hot. By addition of 30 cm^3 of water containing 0.49 g (3 mmol) of NH_4PF_6 a yellow precipitate was obtained. It was filtered, washed with 50 cm^3 of cold water, and dried overnight. The solid was washed copiously with diethyl ether and dried again. It was then dissolved in acetone (20 cm^3), and diethyl ether (ca. 40 cm^3) was added slowly until a yellow solid was obtained. The compound was washed with diethyl ether and dried over P_4O_{10} under vacuum. Yield 0.165 g (50%). − Selected IR data (KBr): $\tilde{\nu}$ = 1619 br, 1577 s, 1549 s, 1167 s, 1127 s, 847 br, 768 s, 754 vs, 723 s, 558 vs cm^{-1}. − $C_{29}H_2F_{12}N_9P_2RuS_3$ (986.76): calcd. C 35.30, H 2.55, N 12.80, S, 9.75; found C 35.30, H 2.60, N 12.75, S 9.80. − Conductivity: Λ_M(MeCN, 2 × 10^{-4} mol dm^{-3}, 20 °C) = 270 S cm^2 mol^{-1}.

$[Ru(dprs)_2(L_2)][PF_6]_2$: The compound was obtained in the same way as the previous complex, starting from $[Ru(dprs)_2Cl_2]\cdot 2H_2O$ (0.196 g, 0.33 mmol) and **L_2** (0.208 g, 0.882 mmol). Yield 0.160 g (48%). − Selected IR data (KBr): $\tilde{\nu}$ = 1579 vs 1549 vs, 1492 s, 1396 vs, 1167 vs, 847 br, 768s, 754 vs, 558 vs cm^{-1}. − $C_{28}H_{22}ClF_{12}N_9P_2RuS_3$ (1007.18): calcd. C 33.40, H 2.20, N 12.50, S 9.55; found C 33.40, H 2.25, N 12.40, S 9.60. − Conductivity: Λ_M(MeCN, 2 × 10^{-4} mol dm^{-3}, 20 °C) = 290 S cm^2 mol^{-1}.

$[Ru(dprs)_2(L_4)][PF_6]_2$: The crude product was prepared in the same way as above, starting from $[Ru(dprs)_2Cl_2]\cdot 2H_2O$ (0.196 g, 0.333 mmol) and **L_4** (0.216 g, 0.666 mmol). The solid was dissolved in acetone (10 cm^3) and added to the top of a chromatography column (diameter 2 cm) packed with aluminium oxide [60 g; Aldrich, neutral, STD grade, 150 mesh, deactivated with water (2.4 g)]. The first orange band was eluted with acetone/CH_2Cl_2 (3:2) (60 cm^3) and acetone (ca 300 cm^3). The orange solid obtained by removal of the solvent was collected and washed with diethyl ether. Further elution with acetone (ca. 400 cm^3) gave a yellow band, which was concentrated (10 cm^3) and precipitated with diethyl ether (90 cm^3). The yellow solid obtained was washed copiously with diethyl ether and dried over P_4O_{10} under vacuum. Yield 0.140 g (30%). − Selected IR data (KBr): $\tilde{\nu}$ = 1617 br, 1577 vs, 1549 vs, 1511 ms, 1167 vs, 846 vs, 766 s, 754 vs, 723 ms, 558 vs cm^{-1}. − $C_{34}H_{28}F_{12}N_{10}P_2RuS_4$ (1095.91): calcd. C 37.25, H 2.60, N 12.80, S 11.70; found C 37.20, H 2.65, N 12.65, S 11.65. − Conductivity: Λ_M(MeCN, 2 × 10^{-4} mol dm^{-3}, 20 °C) = 295 S cm^2 mol^{-1}.

$[Ru(dps)_2(L_1)][PF_6]_2$: The compound was obtained in the same way as above, starting from $[Ru(dps)_2Cl_2]\cdot 2H_2O$ (0.195 g, 0.33 mmol) and **L_1** (0.190 g, 0.882 mmol). Yield 0.163 g (50%). − Selected IR data (KBr): $\tilde{\nu}$ = 1641 br, 1586 s, 1556 s, 1284 s, 1162 s, 1127 s, 845 br, 766 vs, 741 ms, 725 s, 558 vs cm^{-1}. − $C_{33}H_{29}F_{12}N_5P_2RuS_3$ (982.81): calcd. C 40.35, H 2.95, N 7.15, S 9.80; found C 40.40, H 3.00, N 7.05, S 9.85. − Conductivity: Λ_M(MeCN, 2 × 10^{-4} mol dm^{-3}, 20 °C) = 304 S cm^2 mol^{-1}.

$[Ru(dps)_2(L_2)][PF_6]_2$: The compound was obtained in the same way as above, starting from $[Ru(dps)_2Cl_2]\cdot 2H_2O$ (0.195 g, 0.33 mmol) and **L_2** (0.208 g, 0.882 mmol). Yield 0.134 g (40%). − Selected IR data (KBr): $\tilde{\nu}$ = 1588 vs, 1555 s, 1421 vs, 1284 s, 1163 s, 1129 s, 1087 s, 1063 s, 843 br, 768 vs, 740 ms, 727 s, 558 vs cm^{-1}. − $C_{32}H_{26}ClF_{12}N_5P_2RuS_3$ (1003.23): calcd. C 38.30, H 2.60, N 7.00, S 9.60; found C 38.40, H 2.70, N 7.00, S 9.65. − Conductivity: Λ_M(MeCN, 2 × 10^{-4} mol dm^{-3}, 20 °C) = 295 S cm^2 mol^{-1}.

$[Ru(dps)_2(L_3)][PF_6]_2$: The compound was obtained in the same way as above, starting from $[Ru(dps)_2Cl_2]\cdot 2H_2O$ (0.195 g, 0.33 mmol) and **L_3** (0.208 g, 0.882 mmol). Yield 0.167 g (50%). − Selected IR data (KBr): $\tilde{\nu}$ = 1588 vs, 1555 ms, 1422 vs, 1284 s, 1164 s, 1129 s, 1087 s, 1064 s, 845 br, 768 vs, 740 ms, 727 s, 558 vs cm^{-1}. − $C_{32}H_{26}ClF_{12}N_5P_2RuS_3$ (1003.23): calcd. C 38.30, H 2.60, N 7.00, S 9.60; found C 38.40, H 2.70, N 6.95, S 9.55. − Conductivity: Λ_M(MeCN, 2 × 10^{-4} mol dm^{-3}, 20 °C) = 290 S cm^2 mol^{-1}.

$[Ru(dps)_2(L_5)][PF_6]_2$: NaN_3 (0.0325 g, 0.5 mmol) was dissolved in warm methanol (8 cm^3) and added dropwise to a stirred solution of $[Ru(dps)_2(NO)(NO_2)][PF_6]_2\cdot H_2O$ (0.431 g, 0.5 mmol) in acetone (30 cm^3). The solution colour changed from yellow to dark-red. To the solution, protected from light, was added, after 3 min **L_5** (0.324 g, 1.5 mmol), after 2 min a 70% aqueous solution of HPF_6 (3 cm^3), and again a methanol (8 cm^3) solution of NaN_3 (0.0325 g, 0.5 mmol), dropwise. The mixture was stirred for 2 h, filtered, concentrated (20 cm^3), and the product precipitated with diethyl ether (100 cm^3). The yellow solid obtained was dried over P_4O_{10}, under vacuum, crystallised from acetone (10 cm^3) and diethyl ether (90 cm^3), washed with diethyl ether, and dried again. Yield 0.16 g (33%). − Selected IR data (KBr): $\tilde{\nu}$ = 1590 s, 1455 vs, 1423 s, 1286 s, 1165 s, 1064 s, 846 br, 770 s, 726 ms, 558 vs cm^{-1}. − $C_{32}H_{28}F_{12}N_6P_2RuS_3$ (983.80): calcd. C 39.05, H 2.85, N 8.55, S 9.80; found C 39.00, H 2.90, N 8.55, S 9.70. − Conductivity: Λ_M(MeCN, 2 × 10^{-4} mol dm^{-3}, 20 °C) = 305 S cm^2 mol^{-1}.

$[Ru(dps)_2(L_6)][PF_6]_2$: The complex was obtained in the same way as $[Ru(dps)_2(L_5)][PF6]_2$ using **L_6** (0.355 g, 1.5 mmol) instead of **L_5**. Yield 0.15 g (30%). − Selected IR data (KBr): $\tilde{\nu}$ = 1590 s, 1455 vs, 1422 s, 1286 s, 1164 s, 1064 s, 845 br, 770 s, 726 ms, 558 vs cm^{-1}. − $C_{31}H_{25}ClF_{12}N_6P_2RuS_3$ (1004.22): calcd. C 37.10, H 2.50, N 8.35, S 9.60; found C 37.10, H 2.60, N 8.25, S 9.70. − Conductivity: Λ_M(MeCN, 2 × 10^{-4} mol dm^{-3}, 20 °C) = 305 S cm^2 mol^{-1}.

$[Ru(bipy)_2(L_1)][PF_6]_2$: The compound was obtained in the same way as $[Ru(dps)_2(\mathbf{L_1})][PF_6]_2$, starting from $[Ru(bipy)_2Cl_2]\cdot 2H_2O$ (0.174 g, 0.33 mmol) and **L_1** (0.190 g, 0.882 mmol). Yield 0.153 g (50%). − Selected IR data (KBr): $\tilde{\nu}$ = 1605 vs, 1585 s, 1515 s, 1243 s, 1162 s, 1125 s, 1070 ms, 1046 ms, 850 br, 764 vs, 740 ms, 730 s, 558 vs cm^{-1}. − $C_{33}H_{29}ClF_{12}N_5P_2RuS$ (918.69): calcd. C 43.15, H 3.20, N 7.60, S 3.50; found C 43.10, H 3.30, N 7.50, S 3.55. − Conductivity: Λ_M(MeCN, 2 × 10^{-4} mol dm^{-3}, 20 °C) = 296 S cm^2 mol^{-1}.

Acknowledgments

This work was supported by the Ministero dell'Università e della Ricerca Scientifica e Tecnologica (Murst) of Italy.

[1] G. Bruno, F. Nicolò, S. Lo Schiavo, M. S. Sinicropi, G. Tresoldi, *J. Chem. Soc., Dalton Trans.* **1995**, 17−24.
[2] G. Bruno, F. Nicolò, G. Tresoldi, *Acta Crystallogr., Sect. C* **2000**, *56*, 282−283.
[3] G. Tresoldi, S. Lo Schiavo, P. Piraino, P. Zanello, *J. Chem. Soc., Dalton Trans.* **1996**, 885−892.
[4] D. C. Black, *Aust. J. Chem.* **1967**, *20*, 2101−2107.
[5] G. C. Pappalardo, A. Seminara, *J. Inorganic. Nucl. Chem.* **1976**, *38*, 1993−1995.
[6] A. Forchioni, V. Librando, G. C. Pappalardo, *J. Chem. Soc., Dalton Trans.* **1977**, 638−641.
[7] G. Tresoldi, P. Piraino, E. Rotondo, F. Faraone, *J. Chem. Soc., Dalton Trans.* **1991**, 425−430.
[8] G. Tresoldi, E. Rotondo, P. Piraino, M. Lanfranchi, A. Tiripicchio, *Inorg. Chim. Acta* **1992**, *194*, 233−241.
[9] G. De Munno, G. Bruno, E. Rotondo, G. Giordano, S. Lo Schiavo, P. Piraino, G. Tresoldi, *Inorg. Chim. Acta* **1993**, *208*, 67−75.
[10] F. Nicolò, G. Bruno, G. Tresoldi, *Acta Crystallogr., Sect. C* **1996**, *52*, 2188−2191.
[11] G. Tresoldi, S. Lo Schiavo, P. Piraino, *Inorg. Chim. Acta* **1997**, *254*, 381−385.
[12] R. Chotalia, E. C. Constable, M. J. Hannon, D. A. Thocher, *J. Chem. Soc., Dalton Trans.* **1995**, 3571−3580.
[13] M. Kakoti, A. K. Deb, S. Goswami, *Inorg. Chem.* **1992**, *31*, 1302−1304.
[14] A. Juris, V. Balzani, F. Barigelletti, S. Campagna, P. Belser, A. Von Zelewsky, *Coord. Chem. Rev.* **1988**, *84*, 85−277.
[15] A. Basu, T. G. Kasar, N. J. Sapre, *Inorg. Chem.* **1988**, *27*, 4539−4542.
[16] J. P. Collins, J. P. Sauvage, *Inorg. Chem.* **1986**, *25*, 135−141.
[17] R. Scopelliti, G. Bruno, C. Donato, G. Tresoldi, *Inorg. Chim. Acta* **2001**, *313*, 43−55.
[18] G. Binsch, H. Kessler, *Angew. Chem. Int. Ed. Engl.* **1980**, *6*, 411−428.
[19] S. D. Killops, S. A. R. Knox, *J. Chem. Soc., Dalton Trans.* **1978**, 1260 −1269.
[20] S. D. Killops, S. A. R. Knox, G. H. Riding, *J. Chem. Soc., Chem. Commun.* **1978**, 486−488
[21] E. W. Abel, D. Ellis, K. G. Orrell, *J. Chem. Soc., Dalton Trans.* **1992**, 2243−2249.
[22] E. W. Abel, P. J. Heard, K. G. Orrell, M. B. Hursthouse, M. A. Mazid, *J. Chem. Soc., Dalton Trans.* **1993**, 3795−3801.
[23] E. W. Abel, S. K. Bhargava, K. G. Orrell, *Prog. Inorg. Chem.* **1984**, *32*, 1−118.
[24] C. Chachaty, C. Pappalardo, C. G. Scarlata, *J. Chem. Soc., PerkinTrans. 2* **1976**, 1234−1238.

Received May 15, 2001
[I01170]